

Efficient generation and sorting of orbital angular momentum eigenmodes of light by thermally tuned q -plates

Ebrahim Karimi,^{1,2} Bruno Piccirillo,^{1,3} Eleonora Nagali,⁴ Lorenzo Marrucci,^{1,2} and Enrico Santamato^{1,3,a)}

¹*Dipartimento di Scienze Fisiche, Università di Napoli "Federico II," Compl. Univ. di Monte S. Angelo, 80126 Napoli, Italy*

²*Consiglio Nazionale delle Ricerche-INFN Coherentia, 80126 Napoli, Italy*

³*Consorzio Nazionale Interuniversitario per le Scienze Fisiche della Materia, 80126 Napoli, Italy*

⁴*Dipartimento di Fisica, Università di Roma "La Sapienza," 00185 Roma, Italy*

(Received 30 April 2009; accepted 23 May 2009; published online 12 June 2009)

We present methods for generating and for sorting specific orbital angular momentum (OAM) eigenmodes of a light beam with high efficiency, using a liquid crystal birefringent plate with unit topological charge known as " q -plate." The generation efficiency has been optimized by tuning the optical retardation of the q -plate with temperature. The measured OAM $m = \pm 2$ eigenmodes generation efficiency from an input TEM₀₀ beam was of 97%. Mode sorting of the two input OAM $m = \pm 2$ eigenmodes was achieved with an efficiency of 81%. © 2009 American Institute of Physics. [DOI: 10.1063/1.3154549]

A light beam has two "rotational" degrees of freedom: spin angular momentum (SAM) and orbital angular momentum (OAM). Light SAM is related to the vectorial properties of the transverse electric field and may take two values $s = +1$ and $s = -1$ (in units of \hbar), corresponding to left and right circularly polarized light, respectively. Light OAM is defined by the phase structure of the complex electric field^{1,2} and may take any of the infinite values $m = 0, \pm 1, \pm 2, \dots$. In the last decade, the interest in light beams endowed with OAM has continuously increased because of the wide range of scientific and technological applications in both classic³ and quantum regimes of light.^{4,5} Until today, few tools have been developed for generating and manipulating OAM, including pitchfork holograms,⁶ spiral phase plates,^{7,8} Dove prisms eventually inserted in interferometers,⁹ and cylindrical lens mode converters.¹⁰ All these devices and techniques have drawbacks and limitations in terms of efficiency, modulation speed, working wavelength, alignment, and constraints imposed on the input and output beams.

Recently, a further optical device for OAM manipulation has been introduced, made as a birefringent liquid crystal plate having an azimuthal distribution of the local optical axis in the transverse plane, with a topological charge q at its center defect, hence named " q -plate" (QP).^{11,12} When a light beam traverses a QP, the topological charge $2q$ is transferred into the phase of the beam, which thus gains a corresponding amount of OAM, with a sign determined by the light input polarization. In this paper we consider only QPs with $q = 1$, having cylindrical symmetry around their central defect. Because of this symmetry, a $q = 1$ QP cannot change the total SAM+OAM angular momentum of the incident beam, so that its action is just that of converting the SAM variation of some photons into OAM, and vice versa (SAM-to-OAM conversion, or STOC).¹¹ Besides the topological charge q , the QP is characterized by its birefringent retardation δ , ideally uniform in the transverse plane, which determines the STOC efficiency, i.e., the fraction of photons (or optical en-

ergy) that is actually converted.¹³ In this work, we achieved STOC efficiencies exceeding 95%, to be compared, for example, with the record efficiencies ranging from 50% to 90%, depending on the wavelength of computer-generated blazed fork holograms.^{14,15} High efficiencies in producing and detecting the light OAM are highly desirable in all circumstances where only few photons are available. Examples are weak signals coming from far sources, such as the astronomical ones,¹⁶ or after propagation in highly absorbing media, or in quantum information applications. Achieving high efficiencies, however, requires accurate tuning of the QP retardation δ . In order to tune the optical retardation δ and thus optimize the QP efficiency, in this work we adopted a method based on controlling the material temperature, which presents good features in terms of a realization simplicity and stability of the obtained retardation.

This paper is divided in two parts, the first dealing with OAM generation and the second with OAM sorting, e.g., for detection purposes. In the first experiment, we used the STOC process for transforming an input TEM₀₀ laser beam into a beam having OAM $m = \pm 2$. Our QP was manufactured as a 6 μm thick film of E7 liquid crystal from Merck, sandwiched between two circularly rubbed glass substrates coated with a polyimide. The transmittance T of our QP was measured to be 88%, with the losses arising from scattering due to manufacturing imperfections and from the lack of antireflection coating on the cell bounding glasses. The optical setup used to measure the STOC efficiency of our QP as a function of its optical retardation is shown in Fig. 1. The input light was a linearly polarized TEM₀₀ laser beam with a wavelength of 532 nm. After changing the polarization into left-circular (L) by a quarter wave plate (QWP), the beam was made to pass through our controlled-temperature QP. For arbitrarily tuned QPs, the transverse intensity pattern of the beam emerging from the QP is made up of a central spot, corresponding to the fraction of photons whose state is left unchanged (OAM $m = 0$ and L -polarization), surrounded by a single ring, corresponding to the fraction of photons suffering the STOC process and emerging in the state OAM m

^{a)}Electronic mail: enrico.santamato@na.infn.it.

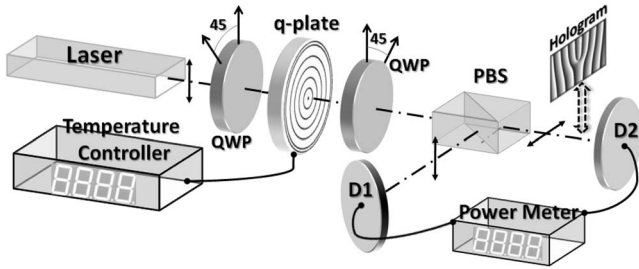


FIG. 1. Setup to measure the STOC efficiency and the state purity. Legend: QWP-quarter wave plate, PBS-polarizing beam-splitter. The fork hologram was inserted on the converted beam arm for verifying the degree of purity of the OAM $m=2$ mode generated on the output.

$=2$ and with right-circular (R) polarization. By inserting in the output beam a second QWP and a polarizing beam-splitter (PBS) oriented so as to select the R -polarization for the transmission output, a pure doughnut beam is obtained. The reflected output of the PBS shows instead only the central spot (unconverted light). If P_{in} is the total input power, the powers of the coherently converted and unconverted components, $P_{R,2}$ and $P_{L,0}$, respectively, are expected to depend on the optical retardation δ according to the following Malus-like laws:^{13,17}

$$P_{R,2} = P_0 \sin^2 \frac{\delta}{2} P_{L,0} = P_0 \cos^2 \frac{\delta}{2}, \quad (1)$$

where $P_0 = TP_{in}$ is the total power transmitted coherently by the QP. To adjust the retardation δ , the temperature of the QP was varied while measuring the power of the two output beams of the PBS. The results are shown in Fig. 2, together with best-fit curves based on Eq. (1), assuming a second-order polynomial dependence $\delta(T) = a + bT + cT^2$ and adding a constant offset of 0.5% that accounts for the finite PBS and wave plates contrast ratios. When the PBS-transmitted power (full squares in Fig. 2) reaches its maximum, we obtain the optimal STOC and almost all photons emerge in the $m=2$ OAM state. More precisely, in this optimal situation, about 99.2% of the beam power is transmitted by the PBS, and after taking into account the finite contrast ratio of the wave plates and PBS (as measured without the QP), the actual QP efficiency in inverting the optical polarization is estimated to be 99.6%. To test the purity of the OAM eigenmode generated by our QP at the optimal temperature, we inserted along the beam a double pitchfork hologram as OAM mode splitter,^{6,14} and on the first-order diffracted beam we selected the central spot by a suitable iris placed before the detector.

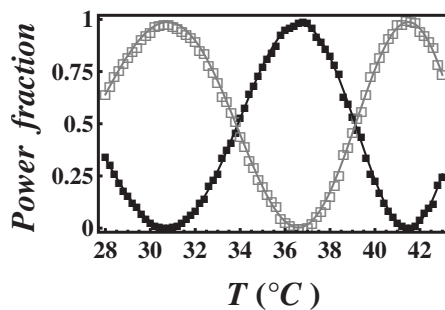


FIG. 2. STOC power fraction $P_{R,2}/P_0$ (black squares) and no STOC power fraction $P_{L,0}/P_0$ (empty squares) as functions of the QP temperature. The curve is the best fit obtained as explained in the text.

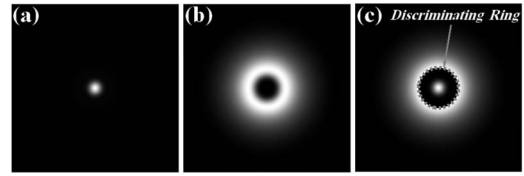


FIG. 3. Calculated far-field patterns of OAM modes $m=0$ and $m=4$ generated by the QP for input OAM $m = \pm 2$ [the input beam was assumed to HyGG_{-2,±2}($r, \phi, 0, 1$) (Ref. 18) mode]. The dashed circle shows the discriminating area used in the balanced mode sorter.

After suitable calibration of the detection efficiency, the measured OAM $m=2$ mode content fraction was estimated to be $F=97.2\%$ (in quantum optics, F is the “fidelity,” i.e., the overlap with the desired mode $m=2$), so that the overall QP efficiency in generating a pure OAM $m=2$ mode is $\eta = 97.2\% \times 99.6\% = 96.9\%$. This value is net of reflection and scattering losses in the QP. If all losses are included, the efficiency of our QP is 85%, a figure which could be easily improved to more than 90% by simply adding antireflection coatings. Moreover, we note that unlike all other methods for OAM generation, the QP approach enables also a very fast (gigahertz) switching of the OAM sign, by electro-optical control of the input polarization.

Let us now discuss the second experiment about OAM mode sorting. More precisely, we present a setup for sorting the four modes that are obtained by combining the two OAM modes $m=2$ and $m=-2$, and the two orthogonal polarizations L and R . The setup is the same as the previous one. The optical retardation of the QP was held fixed at the optimal value $\delta = \pi$ for maximum STOC efficiency and the input states $m = \pm 2$ were generated by an SLM driven with a pitchfork computer generated hologram (CGH). The first QWP was rotated so as to produce, alternately, right-circular and left-circular polarizations. In this way, we created in sequence the four photon states $|L, 2\rangle$, $|L, -2\rangle$, $|R, 2\rangle$, $|R, -2\rangle$. Because the STOC process is complete in a tuned QP, after passing through the QP these four states are expected to change, respectively, into $|R, 4\rangle$, $|R, 0\rangle$, $|L, 0\rangle$, $|L, -4\rangle$. The QWP after the QP, changes these states into $|H, 4\rangle$, $|H, 0\rangle$, $|V, 0\rangle$, $|V, -4\rangle$, respectively, so that the two states $|H, 4\rangle$ and $|H, 0\rangle$ are transmitted by the PBS, and the other two states $|V, 0\rangle$ and $|V, -4\rangle$ are reflected. We see that owing to the QP, the two states in each of the reflected and transmitted beam have different values of the photon OAM ($m=0$ and $m=4$). After propagating in the far-field (or in the focal plane of a lens), these two modes can then be separated by exploiting their different radial distribution, i.e., a central spot for $m=0$ and an outer ring for $m=4$, as shown in Fig. 3, thus finally sorting all four initial spin-orbit modes into separate beams. The radial sorting can be obtained, for example, by means of a mirror with a hole at its center. The efficiency of this mode sorter is defined here as the fraction of the optical power of the eigenmode to be sorted that is directed in the *correct* output mode. This efficiency, however, is not 100% because of the radial mode overlap, leading to some energy going into the “wrong” OAM output mode. This also leads to a finite contrast ratio, i.e., to cross-talk between the input channels. In Table I we report the measured efficiencies and contrast ratios for the four input spin-orbit base states previously mentioned, with a discriminating hole radius chosen so as to balance the output efficiencies for opposite input OAM

TABLE I. The QPs efficiency as a mode sorter.

Input state	Output state	Efficiency	Extinction ratio
$ L, 2\rangle$	$ R, 4\rangle$	81.1%	$\approx 4.6:1$
$ L, -2\rangle$	$ R, 0\rangle$	81.8%	$\approx 4.5:1$
$ R, 2\rangle$	$ L, 0\rangle$	81.6%	$\approx 4.7:1$
$ R, -2\rangle$	$ L, -4\rangle$	81.5%	$\approx 4.6:1$

(see Fig. 3). The extinction ratio due to radial overlap between $m=0$ and $m=4$ OAM modes can be improved by introducing a suitable opaque belt mask that cuts away the overlapping region of the two modes, although at the expense of a reduced efficiency. In principle, the contrast ratio can be made arbitrarily large. Theoretically, we estimate a contrast ratio $>10^3$ for an efficiency of about 50% and $>10^6$ for an efficiency of 10%.¹⁹ Increasing the contrast ratio at the expense of efficiency can be useful in many quantum optics applications where good fidelity is required.²⁰ We note that the radial overlap problem leading to cross-talk is not unique of the QP approach. A similar problem and an equivalent efficiency/contrast ratio tradeoff is also present with hologram-based OAM sorting. We also tested our QP mode sorter with coherent superpositions of $m=+2$ and $m=-2$ OAM modes (obtained with suitable CGHs), obtaining results consistent with the efficiencies reported in Table I.

In conclusion, we demonstrated the application of a liquid crystal QP as (i) a switchable OAM generator and (ii) a OAM mode sorter, exploiting the optical STOC process. By suitable thermal tuning of the birefringent retardation in the QP, we optimized its generation or mode sorting efficiency, finding values as large as $\approx 97\%$ as mode generator and $\approx 81\%$ as mode sorter. These results show that the QPs can easily reach much larger efficiencies than holographic elements and will therefore provide the most convenient option

for many applications, particularly when low photon fluxes are available.

- ¹L. Allen, S. M. Barnett, and M. J. Padgett, *Optical Angular Momentum* (Institute of Physics, Bristol, 2003).
- ²S. Franke-Arnold, L. Allen, and M. J. Padgett, *Laser Photonics Rev.* **2**, 299 (2008).
- ³G. Gibson, J. Courtial, M. J. Padgett, M. Vasnetsov, V. Pasko, S. M. Barnett, and S. Franke-Arnold, *Opt. Express* **12**, 5448 (2004).
- ⁴A. Mair, A. Vaziri, G. Welhs, and A. Zeilinger, *Nature (London)* **412**, 313 (2001).
- ⁵G. Molina-Terriza, J. P. Torres, and L. Torner, *Nat. Phys.* **3**, 305 (2007).
- ⁶V. Y. Bazhenov, M. V. Vasnetsov, and M. S. Soskin, *JETP Lett.* **52**, 429 (1990).
- ⁷M. W. Beijersbergen, R. P. C. Coerwinkel, M. Kristensen, and J. P. Woerdman, *Opt. Commun.* **112**, 321 (1994).
- ⁸K. Sueda, G. Miyaji, N. Miyanaga, and M. Nakatsuka, *Opt. Express* **12**, 3548 (2004).
- ⁹J. Leach, J. Courtial, K. Skeldon, S. M. Barnett, S. F. Arnold, and M. J. Padgett *Phys. Rev. Lett.* **92**, 013601 (2004).
- ¹⁰L. Allen, M. W. Beijersbergen, R. J. C. Spreeuw, and J. P. Woerdman, *Phys. Rev. A* **45**, 8185 (1992).
- ¹¹L. Marrucci, C. Manzo, and D. Paparo, *Phys. Rev. Lett.* **96**, 163905 (2006).
- ¹²L. Marrucci, C. Manzo, and D. Paparo, *Appl. Phys. Lett.* **88**, 221102 (2006).
- ¹³E. Karimi, B. Piccirillo, L. Marrucci, and E. Santamato, *Opt. Lett.* **34**, 1225 (2009).
- ¹⁴N. R. Heckenberg, R. McDuff, C. P. Smith, H. Rubinsztein-Dunlop, and M. J. Wegener, *Opt. Quantum Electron.* **24**, S951 (1992).
- ¹⁵H. He, N. R. Heckenberg, and H. Rubinsztein-Dunlop, *J. Mod. Opt.* **42**, 217 (1995).
- ¹⁶M. Harwit, *Astrophys. J.* **597**, 1266 (2003).
- ¹⁷L. Marrucci, *Mol. Cryst. Liq. Cryst.* **488**, 148 (2008).
- ¹⁸E. Karimi, G. Zito, B. Piccirillo, L. Marrucci, and E. Santamato, *Opt. Lett.* **32**, 3053 (2007).
- ¹⁹The belt mask has the same function of the Lyot stop in optical vortex astronomical coronagraph, see G. A. Swartzlander, Jr., E. L. Ford, R. S. Abdul-Malik, L. M. Close, M. A. Peters, D. M. Palacios, and D. W. Wilson, *Opt. Express* **16**, 10200 (2008).
- ²⁰J. Leach, B. Jack, J. Romero, M. Ritsch-Marte, R. W. Boyd, A. K. Jha, S. M. Barnett, S. Franke-Arnold, and M. J. Padgett, *Opt. Express* **17**, 8287 (2009).